Available online at www.sciencedirect.com

ScienceDirect

IFAC Papers Online CONFERENCE PAPER ARCHIVE

IFAC PapersOnLine 59-1 (2025) 349–354

A metapopulation SIHURD model ⋆

Ion Bica * **Zhichun Zhai** * **Rui Hu** * **Wanhua Su** *

* *MacEwan University, 10700-104 Ave NW, Edmonton, AB, T5J 4S2, Canada (e-mails: bicai@macewan.ca, zhaiz2@macewan.ca, hur3@macewan.ca, suw3@macewan.ca).*

Abstract: We enhance our SIHURD model published in Bica et-al (2022) and propose a metapopulation infectious disease mathematical monitoring model where individuals move between discrete spatial patches. We divide the environment into a finite number of spatial patches (e.g., adjacent cities), which preserve homogeneity characteristics. We apply the enhanced SIHURD model presented in this article to each spatial patch.
The novelty of this model lies in introducing parameters that represent individuals' travel rates between spatial patches, which depend on their disease status. In addition, it assumes that individuals do not change their disease status while travelling between patches.
Our study uses the reproduction number, R_{0_k}, for each spatial patch, $k = 1, 2, \ldots, n, (n > 1)$ integer, which represents the average number of secondary cases produced by an infected individual in a susceptible population. The system has only a disease-free equilibrium point if $R_{0_k} \leq 1$. In contrast, if $R_{0_k} > 1$, the system has an endemic equilibrium point. Reproduction numbers R_{0_k} are crucial for understanding the spread of infectious diseases and can inform measures to control outbreaks effectively.
Migration between patches fundamentally alters the behaviour of the endemic equilibrium within a patch, rendering it unstable in the proposed model.

Copyright © 2025 The Authors. This is an open access article under the CC BY-NC-ND license (https://creativecommons.org/licenses/by-nc-nd/4.0/)

Keywords: Mathematical Model Formulation, Simulation and Visualization, Disease Control, Hospitalization and Critical Care Monitoring, Healthcare Management Policy.

1. INTRODUCTION

The SIR model

$$S' = -\beta SI,\ I' = \beta SI - \gamma_I I,\ R' = \gamma_I I, \tag{1}$$

presented in Ross (1916) and Kermack et-al (1927) is the classical model for studying the dynamics of microparasitic infections (i.e., caused by bacteria or viruses). Here, $S(t)$, $I(t)$, and $R(t)$ represent the number of susceptible, infected, and recovered individuals at time t, respectively. The parameter β represents the transmission rate of the disease, and γ_I indicates the recovery rate of the infected individuals.

In our article Bica et-al (2022) we proposed a model addressing the "acute epidemicity" of infectious disease, and we successfully followed the expected findings in Ross et-al (1917) looking for solutions whose graphs "are bell-shaped and nearly symmetrical and tend to decline more slowly than they rose." In Ross (1916), the author gave a relevant and intuitive classification of infectious diseases, classifying pandemic-type diseases based on their "acute epidemicity" separately from other infectious diseases.

The model (1) is a compartmentalized model manifesting in one spatial patch, i.e., no spatial separation, where the three compartments, S, I, and R, are assumed to be homogeneously mixed, i.e., there are no separations amongst the three compartments at any time.

Arino et-al (2003A) developed a multi-city compartmental epidemic model to analyze disease spread across multiple urban centers interconnected through travel. Also, Arino et-al (2003B) developed a mathematical framework to study the spread of infectious diseases across multiple cities interconnected through travel. Each city was modelled using a susceptible-infectious-recovered (SIR) compartmental structure, with additional terms accounting for travel between cities. Arino et-al (2005) developed a mathematical model to examine the spatial spread of diseases transmissible between multiple species. The model integrates a susceptible-exposed-infectious-recovered (SEIR) framework for each species within distinct spatial regions, referred to as patches. These patches are interconnected through species movement, represented as a directed graph where vertices signify patches and arcs depict movement pathways.

Arino et-al (2006) examined the dynamics of infectious diseases within metapopulation networks of distinct populations (or patches) interconnected through individual movement. They developed mathematical models to understand how disease transmission is influenced by factors such as travel between patches, local disease dynamics, and the heterogeneity of populations.

Jin et-al (2005) developed a mathematical model to examine how population movement between two distinct regions influences disease transmission dynamics. Salmani et-al (2006) developed a mathematical model to examine how diseases spread across different regions, or "patches,"

⋆ Thematic area funding grant. Theme: health and wellness in communities. Office of Research Services, MacEwan University, (2024).

2405-8963 Copyright © 2025 The Authors. This is an open access article under the CC BY-NC-ND license.
Peer review under responsibility of International Federation of Automatic Control.
10.1016/j.ifacol.2025.03.060

with varying travel rates for individuals based on their disease status. Wang et-al (2003) developed a susceptible-infected-susceptible (SIS) model to examine how population dispersal between distinct regions, or "patches," influences disease dynamics. Wang et-al (2004) developed a mathematical model to examine how population dispersal among distinct regions, or "patches," influences the spread of infectious diseases.

Motivated by the above-mentioned works, we will introduce a metapopulation SIHURD model.

2. MODEL SET-UP

The new model that we propose builds on the SIHURD model proposed in Bica et-al (2022) and is the following system of differential equations, a metapopulation susceptible - infected - hospitalized - (intensive care) unit - recovered - deceased model (MSIHURD) applicable to each spatial patch $k = 1 \cdots n$, $n > 1$:

$$\begin{aligned}
S_k' &= \tau N_k - \frac{\beta_k}{N_k} S_k I_k - \tau S_k + \sum_{j=1}^{n} \left(s_{kj} - s_{jk}\right) S_k, \\
I_k' &= \frac{\beta_k}{N_k} S_k I_k - (\gamma_{I_k} + \nu_k + \eta_k + \mu_{I_k} + \tau) I_k \\
&\quad + \sum_{j=1}^{n} \left(i_{kj} - i_{jk}\right) I_k, \\
H_k' &= \nu_k I_k - (\tau + \gamma_{H_k} + \mu_{H_k}) H_k, \\
U_k' &= \eta_k I_k - (\tau + \gamma_{U_k} + \mu_{U_k}) U_k, \\
R_k' &= \alpha_{I_k}\gamma_{I_k} I_k + \alpha_{H_k}\gamma_{H_k} H_k + \alpha_{U_k}\gamma_{U_k} U_k - \tau R_k \\
&\quad + \sum_{j=1}^{n} \left(r_{kj} - r_{jk}\right) R_k, \\
D_k' &= \mu_{I_k} I_k + \mu_{H_k} H_k + \mu_{U_k} U_k - d D_k.
\end{aligned} \tag{2}$$

- $S_k(t)$, $I_k(t)$, $H_k(t)$, $U_k(t)$, $R_k(t)$, and $D_k(t)$ represent the number of susceptible, infected, hospitalized (no intensive care unit - ICU), ICU hospitalized individuals, recovered, and deceased individuals (cumulative) due to the infection at time t in patch k.
- N_k : population size in patch k.
- β_k : transmission rate of disease from an infected individual to a susceptible individual in patch k.
- τ : natural mortality rate of human individuals assumed constant for each patch.
- s_{mp}, i_{mp}, and r_{mp}, $m = 1 \cdots n$, $p = 1 \cdots n$, $m \neq p$: rate of individuals migrating from patch p to patch m, and registered as susceptible, infected, and recovered in patch m, respectively.
- γ_{I_k}, γ_{H_k}, and γ_{U_k} : global average recovery rate overall infected, hospitalized (no ICU), and hospitalized (ICU) individuals in patch k, respectively.
- α_{I_k} : dimensionless multiple of γ_{I_k} indicating the expected recovery rate of each infected individual specific to the unit of time used. $\alpha_{I_k} \in (0, 1]$, with $\alpha_{I_k} = 1$ when the recovery of an infected individual from the compartment I_k is completed in patch k.
- α_{H_k} : dimensionless multiple of γ_{H_k} indicating the expected recovery rate of each infected individual specific to the unit of time used. $\alpha_{H_k} \in (0, 1]$, with $\alpha_{H_k} = 1$ when the recovery of an infected individual from the compartment H_k is completed in patch k.
- α_{U_k} : dimensionless multiple of γ_{U_k} indicating the expected recovery rate of each infected individual specific to the unit of time used. $\alpha_{U_k} \in (0, 1]$, with $\alpha_{U_k} = 1$ when the recovery of an infected individual from the compartment U_k is completed in patch k.
- ν_k : rate of infected individuals who need to be hospitalized (no ICU) in patch k.
- η_k : proportion of infected individuals requiring ICU admission in a given patch k.
- μ_{I_k}, μ_{H_k}, and μ_{U_k} : microparasitic-induced averaged fatality rate of infected individuals, hospitalized (no ICU), and hospitalized (ICU) individuals in patch k, respectively.
- $1/d$: mean caring duration of deceased human individuals. d denotes the burial rate of deceased human individuals, and we assume that $d \geq \tau$ for each patch.

The MSIHURD model (2) takes into account the following assumptions:

It has vital dynamics, see Hethcote (2000): death balances the birth at a constant rate τ in each patch k, so we take into account the inflow of newborns into the susceptible compartment at rate τN_k and deaths in the compartments S_k, I_k, H_k, U_k, and R_k at rates τS_k, τI_k, τH_k, τU_k, and τR_k respectively. We also assume infants can experience microparasitic infection, see Kam et-al (2020).

The system is not closed because we take into account the burial rate, d. Thus, the rate at which the total population varies for each patch k, is given by

$$\begin{aligned}
&\frac{d}{dt}\left(S_k + I_k + H_k + U_k + R_k + D_k\right) \\
&= \tau\left[N_k - (S_k + I_k + H_k + U_k + R_k)\right] \\
&-\gamma_{I_k}\left(1 - \alpha_{I_k}\right) I_k - \gamma_{H_k}\left(1 - \alpha_{H_k}\right) H_k - \gamma_{U_k}\left(1 - \alpha_{U_k}\right) U_k \\
&+ \sum_{j=1}^{n} \left[\left(s_{kj} - s_{jk}\right) S_k + \left(i_{kj} - i_{jk}\right) I_k + \left(r_{kj} - r_{jk}\right) R_k\right] - d D_k.
\end{aligned}$$

Without the burial rate d, when all infected population is recovered, i.e., $\alpha_{I_k} = \alpha_{H_k} = \alpha_{U_k} = 1$, and considering the system (2) with $N_k = S_k(t) + I_k(t) + H_k(t) + U_k(t) + R_k(t)$, $k = 1, 2, \ldots, n$, then the system is closed. Indeed, we have:

$$\begin{aligned}
&\frac{d}{dt} \sum_{k=1}^{n} \left(S_k + I_k + H_k + U_k + R_k + D_k\right) = 0 \\
&\Rightarrow \sum_{k=1}^{n} \left(S_k + I_k + H_k + U_k + R_k + D_k\right) = constant,
\end{aligned}$$

which proves the consistency of our modelling concerning the SIR classic endemic model Hethcote (2000). Our assumption agrees with the fact that mortality happens regardless of epidemic microparasitic infections.

3. MATHEMATICAL ANALYSIS

Similar to that in Bica et-al (2022), we can deduce that the reproduction numbers, R_{0_k}, for each spatial patch $k = 1, 2, \ldots, n$, $n > 1$, of a microparasitic infection modeled by system (2) can be defined as follows:

$$R_{0_k} = \frac{\beta_k}{\gamma_{I_k} + \nu_k + \eta_k + \mu_{I_k} + \tau}. \tag{3}$$

For more information regarding the reproduction number see van den Driessche et-al (2002).

In this paper, we are only interested in the case when we have an endemic equilibrium point in each patch, i.e., $R_{0_k} > 1,\ k = 1, 2, \ldots, n,\ n > 1$. For each patch, $k = 1, 2, \ldots, n,\ n > 1$, the MSIHURD model has the following endemic equilibrium point, $(\hat{S}, \hat{I}, \hat{H}, \hat{U}, \hat{R}, \hat{D})$:

$$\hat{S} = \frac{N_k(\beta_k - R_{0_k}\Sigma_{I_k})}{R_{0_k}\beta_k},$$

$$\hat{I} = \frac{N_k(\beta_k(\tau(1 - R_{0_k}) - \Sigma_{S_k}) + R_{0_k}\Sigma_{I_k}(\Sigma_{S_k} - \tau))}{\beta_k(R_{0_k}\Sigma_{I_k} - \beta_k)},$$

$$\hat{H} = \frac{\nu_k\hat{I}}{\sigma_{H_k}},\ \hat{U} = \frac{\eta_k\hat{I}}{\sigma_{U_k}}, \tag{4}$$

$$\hat{R} = \frac{\hat{I}((\alpha_{I_k}\gamma_{I_k}\sigma_{U_k} + \eta_k\alpha_{U_k}\gamma_{U_k})\sigma_{H_k} + \nu_k\alpha_{H_k}\gamma_{H_k}\sigma_{U_k})}{\sigma_{H_k}\sigma_{U_k}(\tau - \Sigma_{R_k})},$$

$$\hat{D} = \frac{\hat{I}((\eta_k\mu_{U_k} + \mu_{I_k}\sigma_{U_k})\sigma_{H_k} + \nu_k\mu_{H_k}\sigma_{U_k})}{d\sigma_{H_k}\sigma_{U_k}},$$

where $\Sigma_{S_k} := \sum_{j=1}^{n}(s_{kj} - s_{jk})$, $\Sigma_{I_k} := \sum_{j=1}^{n}(i_{kj} - i_{jk})$, and $\Sigma_{R_k} := \sum_{j=1}^{n}(r_{kj} - r_{jk})$.

Linearizing the system (2) about its equilibrium point (4), we obtain the following Jacobian matrix, J, representing the coefficient matrix of the linearized system of (2) about its equilibrium point (4):

$$J = \begin{bmatrix} \frac{\tau R_{0_k}\beta_k}{Denom} & \Sigma_{I_k} - \frac{\beta_k}{R_{0_k}} & 0 & 0 & 0 & 0 \\ \frac{Num}{Denom} & 0 & 0 & 0 & 0 & 0 \\ 0 & \nu_k & -\sigma_{H_k} & 0 & 0 & 0 \\ 0 & \eta_k & 0 & -\sigma_{U_k} & 0 & 0 \\ 0 & \alpha_{I_k}\gamma_{I_k} & \alpha_{H_k}\gamma_{H_k} & \alpha_{U_k}\gamma_{U_k} & \Sigma_{R_k} - \tau & 0 \\ 0 & \mu_{I_k} & \mu_{H_k} & \mu_{U_k} & 0 & -d \end{bmatrix}, \tag{5}$$

where we made the following notations:

$$Num := \beta_k\left(\tau(1 - R_{0_k}) - \Sigma_{S_k}\right) + R_{0_k}\Sigma_{I_k}\left(\Sigma_{S_k} - \tau\right),$$
$$\text{and } Denom := R_{0_k}\Sigma_{I_k} - \beta_k.$$

The matrix J has the following eigenvalues:

$$\lambda_{1,2} = \frac{\Omega_{k_\pm}}{2R_{0_k}\omega_k},$$
$$\lambda_3 = -\sigma_{H_k},\ \lambda_4 = -\sigma_{U_k},\ \lambda_5 = \Sigma_{R_k} - \tau,\ \lambda_6 = -d, \tag{6}$$

where we made the following notations:

$$\Omega_{k_\pm} := \tau R_{0_k}^2\beta_k \pm$$
$$\sqrt{\tau^2 R_{0_k}^4\beta_k^2 - 4R_{0_k}\omega_k^2[\tau((R_{0_k} - 1)\beta_k + \Sigma_{I_k}R_{0_k}) - \Sigma_{S_k}\omega_k]},$$

and $\omega_k := R_{0_k}\Sigma_{I_k} - \beta_k$.

The eigenvalues obtained in (6) do not always possess the property that the real part of every eigenvalue is negative; thus, migration between spatial patches will affect the stability of the endemic equilibrium point (4) of the system.

Next, we want to prove that if we start with nonnegative initial conditions for the MSIHURD model (2), all trajectories will reside in $\mathcal{R}_+^6$.

Theorem 1. If $S_k(0) = S_{0_k} \geq 0$, $I_k(0) = I_{0_k} \geq 0$, $H_k(0) = H_{0_k} \geq 0$, $U_k(0) = U_{0_k} \geq 0$, $R_k(0) = S_{0_k} \geq 0$, and $D_k(0) = D_{0_k} \geq 0$ in each patch $k = 1, 2, \ldots, n,\ n > 1$, then the trajectories of the system (2) will reside in $\mathcal{R}_+^6$ within each patch $k = 1, 2, \ldots, n,\ n > 1$.

Proof. The first equation of (2) can be written as

$$S_k'(t) + P_k(t)S_k(t) - Q_k = 0, \tag{7}$$

with $P_k(t) = \frac{\beta_k}{N_k}I_k(t) + \tau - \sum_{j=1}^{n}(s_{kj} - s_{jk}), Q_k = \tau N_k$. The equation (7), under the initial condition $S_k(0) = S_{0_k}$, has the unique solution

$$S_k(t) = e^{-\int_0^t P_k(w)dw}\left(\int_0^t Q_k e^{\int_0^v P_k(w)dw}dv + S_{0_k}\right)$$

which implies immediately that $S_k(t) \geq 0$ for all $t \geq 0$ if $S_{0_k} \geq 0$.

The second equation of the system (2) can be viewed as a separable ordinary differential equation in the variable $I_k(t)$ as follows

$$\frac{I_k'(t)}{I_k(t)} = T_k(t) \tag{8}$$

with

$$T_k(t) = \beta_k\frac{S_k(t)}{N_k} - (\gamma_{I_k} + \nu_k + \eta_k + \mu_{I_k} + \tau) + \sum_{j=1}^{n}(i_{kj} - i_{jk}).$$

The equation (8), under the initial condition $I(0) = I_{0_k}$, has the unique solution $I_k(t) = I_{0_k}e^{\int_0^t T_k(w)dw}$, which implies immediately that $I_k(t) \geq 0$ for all $t \geq 0$, if $I_{0_k} \geq 0$.

Let us prove that $H_k(t) \geq 0$ for all $t \geq 0$. The third equation of the system (2) can be viewed as first-order ordinary differential equations in standard form, as follows

$$H_k'(t) + P_kH_k(t) - Q_k(t) = 0, \tag{9}$$

where $P_k = \tau + \gamma_{H_k} + \mu_{H_k}$, $Q_k(t) = \nu_kI_k(t)$. The equation (9), under the initial conditions $H_k(0) = H_{0_k}$, has the following unique solution

$$H_k(t) = e^{-P_kt}\left(\int_0^t e^{P_kw}Q_k(w)\,dw + H_{0_k}\right). \tag{10}$$

Since $I_k(t) \geq 0$ for all $t \geq 0$, $Q_k(t) \geq 0$ for all $t \geq 0$. If $H_{0_k} \geq 0$, from (10), it immediately follows that $H_k(t) \geq 0$ for all $t \geq 0$. Similarly, we get $U_k(t) \geq 0$ for all $t \geq 0$.

The fifth equation of the system (2) can be written as

$$R_k'(t) + P_kR_k(t) - Q_k(t) = 0, \tag{11}$$

with $Q_k(t) = \alpha_{I_k}\gamma_{I_k}I_k(t) + \alpha_{H_k}\gamma_{H_k}H_k(t) + \alpha_{U_k}\gamma_{U_k}U_k(t)$, $P_k = \tau - \sum_{j=1}^{n}(r_{kj} - r_{jk})$. The equations (11), under the initial conditions $R_k(0) = R_{0_k}$, has the following unique solution

$$R_k(t) = e^{-P_kt}\left(\int_0^t e^{P_kw}Q_k(w)dw + R_{0_k}\right). \tag{12}$$

Since $I_k(t) \geq 0$, $H_k(t) \geq 0$, and $U_k(t) \geq 0$ for all $t \geq 0$, we have $Q_k(t) \geq 0$ for all $t \geq 0$. If $R_{0_k} \geq 0$, and from (12), it follows immediately that $R_k(t) \geq 0$ for all $t \geq 0$.

Similarly, we can prove that $D_k(t) \geq 0$ for all $t \geq 0$.

Hence, under nonnegative initial conditions, the trajectories of the system (2) reside in $\mathcal{R}^6_+$.

3.1 Model Interpretation and Discussions

When we create a mathematical model that describes an infectious disease, typically, we consider the population residing in one spatial patch, with no individuals leaving the patch (except death) and no individuals entering the patch (except birth). The "advantage" of a one-patch scenario in modelling an infectious disease is that the endemic equilibrium point ends up being globally asymptotically stable, which intuitively makes sense; Bica et-al (2022) provides references to such works.

The results of Section 3 are put into the same context as the references mentioned in Section 1 of authors' modelling on multi-spatial patches that also motivated this work. The context is that an infectious disease does not manifest in a closed and homogeneously distributed spatial patch of individuals. Individuals are spread non-uniformly across the surface of the Earth, yet in concentrated spatial patches mainly, and the geographic distance can significantly influence the spread and manifestation of an infectious disease; thus, the benefit of considering this context when modelling an infectious disease with "acute epidemicity." The paper aimed to bring our view and contribution to mathematically modelling an infectious disease when the population is non-uniformly distributed and divided into a finite number of spatial patches (e.g., adjacent cities) that preserve homogeneity characteristics.

Before starting the mathematical analysis of our model, we intuitively predicted that the endemic point of the model should turn out to be unstable, which presents the main difference between the SIHURD model published in Bica et-al (2022) and the MSIHURD model (2) proposed in this article. An example affirming our intuition as to why, in reality, the endemic point of an infectious disease is unstable is the measles breakout that happened in Canada in 2024 but not uniformly throughout each province of Canada; the Public Health of Canada (2024) reported a jump from 12 cases in 2023 to 139 cases in 2024 (information accurate to December 7, 2024, as reported by the agency) with most cases encountered in Quebec (53), New Brunswick (47), and Ontario (36), while Alberta, British Columbia, and Saskatchewan declared only one case each, and no cases reported in the territories. Measles is a well-known microparasitic infection of the human body. Through migration between spatial patches, humans can affect the endemic point of measles in a patch, making it unstable, and thus, measles outbreaks appear.

Our mathematical model (2) is an abstract representation of an infectious disease manifestation, and we used the local theory of nonlinear systems of ordinary differential equations to describe its behaviour.

4. NUMERICAL SIMULATIONS

We use our MSIHURD model (2) to simulate a pandemic-type scenario for a metapopulation consisting of three patches: patch 1: $N_1 = 15000$ individuals, patch 2: $N_2 = 2500$ individuals, and patch 3: $N_3 = 5000$ individuals.

Table 1. Parameters for each patch $k = 1 \dots 3$, measured per time-unit ($t.u.$), with monitoring time considered for the experiment 90 t.u.

Parameters	Values	Data Source (or inspired by)
τ	$1e-05$	WPR (2024)
d	$7.542 \cdot 1e-03$	MacroTrends (2024)
β_k	0.4417	Carcione et-al (2020)
η_k	0.001	assumed
ν_k	0.013	assumed
γ_{I_k}	0.1384	Sen et-al (2021)
γ_{H_k}, γ_{U_k}	0.4, 0.2	assumed
μ_{I_k}	0.00542	Sen et-al (2021)
μ_{H_k}, μ_{U_k}	0.001, 0.008	assumed
α_{I_k}	0.1	Bica et-al (2022)
α_{H_k}, α_{U_k}	$\alpha_{I_k}/2$, $\alpha_{I_k}/4$	Bica et-al (2022)

We assume the following migrating rates between patches: $s_{21} = 15/N_1$, $s_{12} = 5/N_2$, $s_{31} = 8/N_1$, $s_{13} = 6/N_3$, $s_{32} = 3/N_2$, $s_{23} = 12/N_3$, $i_{21} = 19/N_1$, $i_{12} = 4/N_2$, $i_{31} = 15/N_1$, $i_{13} = 10/N_3$, $i_{32} = 3/N_2$, $i_{23} = 6/N_3$, $r_{21} = 19/N_1$, $r_{12} = 4/N_2$, $r_{31} = 15/N_1$, $r_{13} = 12/N_3$, $r_{32} = 3/N_2$, $r_{23} = 10/N_3$.

The initial condition of the system (2) is considered:

$$S_0 = N_{k_{k=1\cdots3}},\ I_0 = 1,\ H_0 = U_0 = R_0 = D_0 = 0. \quad (13)$$

We used the MAPLE software to obtain the numerical solutions of the initial value problem (2, 13) and presented the numerical simulations in this section. We used the same technique as in our paper Bica et-al (2022) as the initial value problem (2, 13) is a stiff problem. We used the Rosenbrock method Shampine (1982) with relative error 10^{-6}, and the returned procedure was called only for points inside the range on which the method evaluated the numerical solution of the system (2) with specified initial conditions. The accuracy of the numerical solutions was also facilitated by increasing the digits environment in MAPLE to 30.

Figure 1 shows the expected behaviour of the susceptible population for each patch $k = 1 \dots 3$. The influence of migration between patches is observed in the compartment S_1 when the number of susceptible individuals initially increases due to migration from the other two patches. Also, the number of susceptible individuals cannot decrease to zero in constancy with the manifestation of infectious diseases, which Figure 1 shows for all three patches.

Figures 2, 3, and 4 illustrate the significant expected behaviour of an infectious disease with acute epidemicity in each patch. All three figures depict the typical pattern of an infectious disease, where the graphs of the solutions "are bell-shaped and nearly symmetrical, and tend to decline more slowly than they rose" Ross et-al (1917).

Figure 5 shows the manifestation of the recovered individuals in each patch, and it follows the expected behaviour of an epidemiological model of an infectious disease. The influence of migration between patches is observed in the compartment R_3 when the number of recovered individuals decreases due to migration to the other two patches.

Figure 6 shows the death compartment of the MSIHURD model, which is consistent with the expected behaviour of an epidemiological model of an infectious disease.

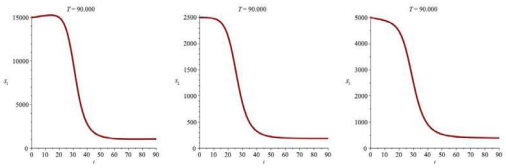

Fig. 1. MSIHURD: Plot of trajectories of the susceptible compartment S_k, $k = 1 \dots 3$.

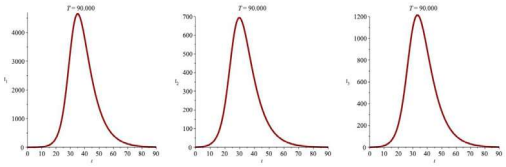

Fig. 2. MSIHURD: Plot of trajectories of the infected compartment I_k, $k = 1 \dots 3$.

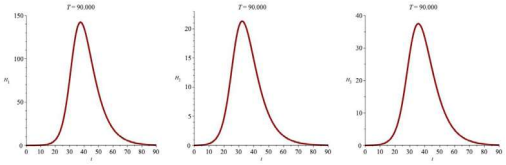

Fig. 3. MSIHURD: Plot of trajectories of the hospitalized (no ICU) compartment H_k, $k = 1 \dots 3$.

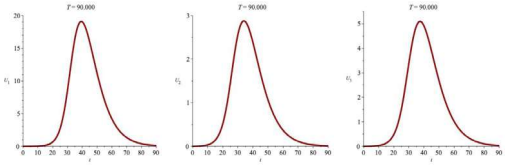

Fig. 4. MSIHURD: Plot of trajectories of the hospitalized (ICU) compartment U_k, $k = 1 \dots 3$.

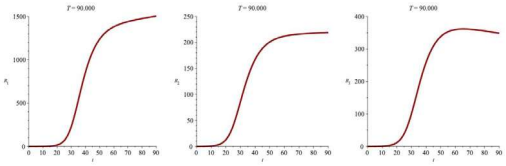

Fig. 5. MSIHURD: Plot of trajectories of the recovered compartment R_k, $k = 1 \dots 3$.

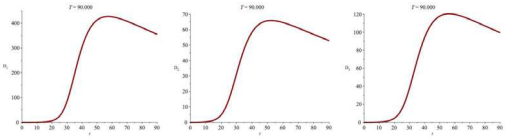

Fig. 6. MSIHURD: Plot of trajectories of the death compartment D_k, $k = 1 \dots 3$.

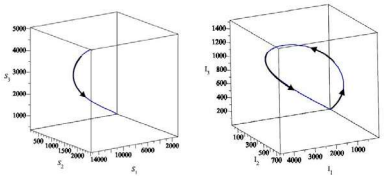

Fig. 7. MSIHURD: The dynamics of the compartments S_k, and I_k between patches $k = 1 \dots 3$, respectively.

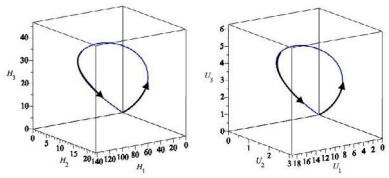

Fig. 8. MSIHURD: The dynamics of the compartments H_k, and U_k between patches $k = 1 \dots 3$, respectively.

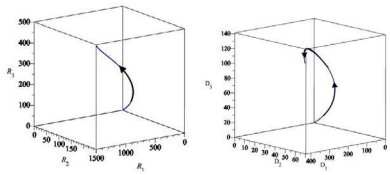

Fig. 9. MSIHURD: The dynamics of the compartments R_k, and D_k between patches $k = 1 \dots 3$, respectively.

Figures 7, 8, & 9 show the nonlinear behaviour of each compartment, S_k, I_k, H_k, U_k, R_k, and D_k over the whole metapopulation, i.e., all three patches $k = 1 \dots 3$. We see a downward trend for the susceptible compartment throughout the infectious disease wave. For the compartments I_k, H_k, and U_k, $k = 1 \dots 3$, we see a consistent increase in the number of infected, hospitalized (no ICU), and hospitalized (ICU) at the beginning of the infection wave, followed by a consistent decrease afterwards. For our experiment, our simulations showed that the downturn point in the evolution of these three compartments happened in the [30, 40] time-unit interval. We also see an upward trend for the recovered compartment throughout the infectious disease wave. The death compartment showed a consistent upward trend, culminating in our simulations around $t = 60$ $t.u.$, followed by a steady decline for the rest of the infection wave.

The numerical simulations presented in this section are important as they demonstrate a consistent system behaviour of the MSIHURD model (2) that aligns with the expected behaviour of a microparasitic infectious disease. This simulation consistency allows us to argue that the system exhibits robust dynamics, even if the endemic point (4) is unstable.

5. CONCLUSIONS

In this article, we proposed the MSIHURD model (2) as a step-up of the SIHURD model that we published Bica et-al (2022) by considering a metapopulation scenario for infectious diseases. The numerical simulations presented in Section 4 are consistent with the expected behaviour of an infectious disease with acute epidemicity.

While the model proposed in our previous work Bica et-al (2022) already included the compartments H, U, and D, and the novelty of the model presented in this article only consists of the introduction of spatial patches, this novelty may prove essential in managing hospitalization, critical care monitoring, and disease control, as each spatial patch may have different needs in terms of how much bed (no ICU) inventory and bed (ICU) inventory is needed in every spatial patch, which in our opinion, it allows a much more effective role taken in managing the infectious disease.

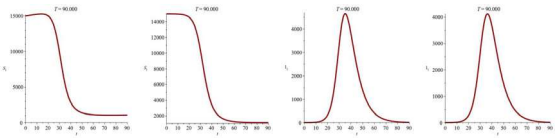

Fig. 10. Trajectories of S_1 and I_1 with migration in effect versus migration rates set to zero, respectively.

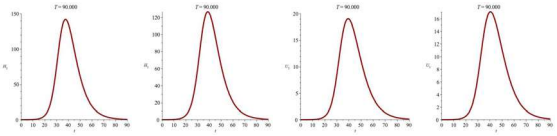

Fig. 11. Trajectories of H_1 and U_1 with migration in effect versus migration rates set to zero, respectively.

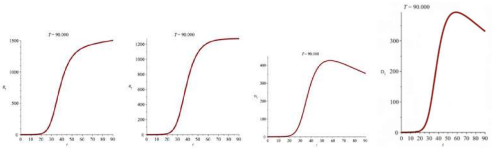

Fig. 12. Trajectories of R_1 and D_1 with migration in effect versus migration rates set to zero, respectively.

In terms of healthcare management policy, the MSIHURD model (2), likewise the SIHURD model proposed in Bica et-al (2022), is intended to be a tool for understanding and better managing the fight against the spread of an infectious disease. By having the necessary information this model can produce, hospitals around the world can create health management policies based on different types of infectious diseases and make better decisions on how to be prepared if an outbreak occurs, being aware at the same time of the populated spatial patches around them and how the migration between patches can affect the spread of an infectious disease. Figures 10, 11, and 12 show the difference in patch 1, for example, between the scenario when the migration rates are in effect (left figure) and the scenario with all migration parameters set to zero (right figure), respectively. By observing the differences in these figures, we believe we have improved the SIHURD model achieved by including spatial patches.

By modelling infectious diseases mathematically, we want to emphasize that we do not need to seek "perfection necessarily" to provide a scenario that may often present an ideological case for a disease manifestation rather than reality. One improvement that we accomplished in proposing the MSIHURD model (2) from our previous model published in Bica et-al (2022) was that the proposed model closes up more to the reality of an infectious disease.

REFERENCES

Arino, J., Davis, J. R., Hartley, D., Jordan, R., Miller, J. M., and van den Driessche, P. (2005). A multi-species epidemic model with spatial dynamics. *Mathematical Medicine and Biology*, 22, 129-142.

Arino, J., and van den Driessche, P. (2003). The basic reproduction number in a multi-city compartmental epidemic model. *Proceedings of Posta*, 294, 135 -142.

Arino, J., and van den Driessche, P. (2003). A multi-city epidemic model. *Mathematical Population Studies*, 10, 175 -193.

Arino, J., and van den Driessche, P. (2006). Disease spread in metapopulation. *Fields Institute Communications*, 48, 1-13.

Bica, I., Zhai, Z., and Hu, R. (2022). A Modified Susceptible-Infected-Recovered Epidemiological Model. *Annals of the University of Craiova, Mathematics and Computer Science Series*, 49(2), 291-308.

Carcione, J. M., Santos, J. E., Bagaini, C., and Ba, J. (2020). A Simulation of a COVID-19 Epidemic Based on a Deterministic SEIR Model. *Front. Public Health*, 8:230.

Hethcote, H. W. (1989). Three basic epidemiological models. *Applied Mathematical Ecology*, 18, 119-144.

Hethcote, H. W. (2000). The mathematics of infectious diseases. *SIAM Review*, 42(4), 599-653.

Jin, Y., and Wang, W. (2005). The effect of population dispersal on the spread of a disease. *Journal of Mathematical Analysis and Applications*, 308, 343 -364.

Kam, K-q., Yung, C. F., Cui, L., Pin Lin, R. T., Mak, T. M., Maiwald, M., Li, J., Chong, C. Y., Nadua, K., Hui Tan, N. W., Thoon, K. C. (2020). A Well Infant With Coronavirus Disease 2019 With High Viral Load. *Clinical Infectious Diseases*, 71(15), 847–849.

Kermack, W. O., McKendrick, A. G. (1927). A contribution to the mathematical theory of epidemics, *Proceedings of the Royal Society of London. Series A, Containing papers of a mathematical and physical character*, 115(772), 700-721.

MacroTrends, Global Matrix, Death Rate (2024). `https://www.macrotrends.net/global-metrics.`

Public Health of Canada - Government of Canada. `https://www.canada.ca/en/public-health.html.`

Ross, R. (1916). An application of the theory of probabilities to the study of a priori pathometry-Part I. *Proceedings of the Royal Society A, Mathematical, Physical and Engineering Sciences*, 92(638), 204-230.

Ross, R., and Hudson, H. P. (1917). An application of the theory of probabilities to the study of a priori pathometry- Part II. *Proceedings of the Royal Society A, Mathematical, Physical and Engineering Sciences*, 93(650), 212-225.

Salmani, M., and van den Driessche, P. (2006). A model for disease transmission in a patchy environment. *Discrete and Continuous Dynamical Systems, Series B*, 6, 185-202.

Sen, D., and Sen, D. (2021). Use of a Modified SIRD Model to Analyze COVID-19 Data. *Ind. Eng. Chem. Res.*, 60(11), 4251-4260.

Shampine, L. F. (1982). Implementation of Rosenbrock methods. *ACM transactions on Mathematical Software*, 8(2), 93-113.

van den Driessche, P., and Watmough, J. (2002). Reproduction numbers and sub-threshold endemic equilibria for compartmental models of disease transmission. *Mathematical Biosciences*, 180, 29-48.

Wang, W., and Mulone, G. (2003). Threshold of disease transmission in a patch environment. *Journal of Mathematical Analysis and Applications*, 85, 321-335.

Wang, W. and Zhao, X. Q. (2004). An epidemic model in a patchy environment. *Mathematical and Bioscience*, 190, 91-112.

WPR: World Population Review (2024). `https://worldpopulationreview.com.`